

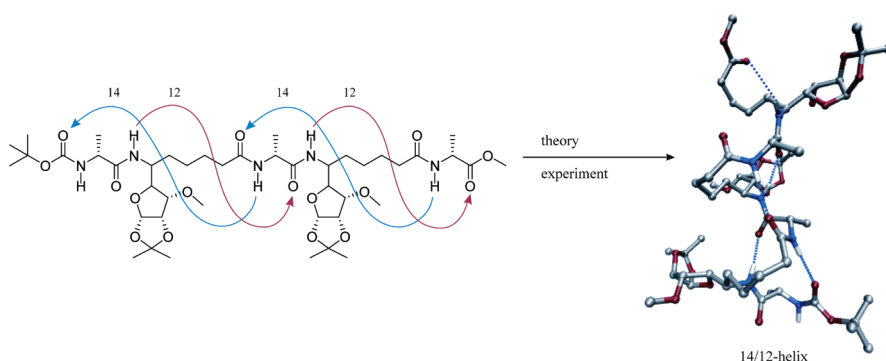
Theoretical and Experimental Studies on α/ϵ -Hybrid Peptides: Design of a 14/12-Helix from Peptides with Alternating (*S*)-C-Linked Carbo- ϵ -amino Acid [(*S*)- ϵ -Caa_(x)] and L-Ala

Gangavaram V. M. Sharma,^{*,†} Bommagani Shoban Babu,[†] Deepak Chatterjee,[‡] Kallaganti V. S. Ramakrishna,[‡] Ajit C. Kunwar,^{*,‡} Peter Schramm,[§] and Hans-Jörg Hofmann^{*,§}

[†]Organic Chemistry Division III, Indian Institute of Chemical Technology (CSIR), Hyderabad 500 607, India, [‡]Centre for Nuclear Magnetic Resonance, Indian Institute of Chemical Technology (CSIR), Hyderabad 500 607, India, and [§]Institute of Biochemistry, Faculty of Biosciences, University of Leipzig, Brüderstrasse 34, D-04103 Leipzig, Germany

esmvee@iict.res.in; kunwar@iict.res.in; hofmann@uni-leipzig.de

Received June 15, 2009



An (*S*)-C-linked carbo- ϵ -amino acid [(*S*)- ϵ -Caa_(x)] was prepared from the known (*S*)- δ -Caa. This monomer was utilized together with L-Ala to give novel α/ϵ -hybrid peptides in 1:1 alternation. Conformational analysis on penta- and hexapeptides by NMR (in CDCl₃), CD, and MD studies led to the identification of robust 14/12-mixed helices. This is in agreement with the data from a theoretical conformational analysis on the basis of ab initio MO theory providing a complete overview on all formally possible hydrogen-bonded helix patterns of α/ϵ -hybrid peptides with 1:1 backbone alternation. The “new motif” of a mixed 14/12-helix was predicted as most stable in vacuum. Obviously, the formation of ordered secondary structures is also possible in peptide foldamers with amino acid constituents of considerable backbone lengths. Thus, α/ϵ -hybrid peptides expand the domain of foldamers and allow the introduction of desired functionalities via the α -amino acid constituents.

Introduction

Peptide foldamer research contributes to a better understanding of folding and function of native peptides

(l) (a) Hill, D. J.; Mio, M. J.; Prince, R. B.; Hughes, T. S.; Moore, J. S. *Chem. Rev.* **2001**, *101*, 3893–4011. (b) Seebach, D.; Matthews, J. L. *Chem. Commun.* **1997**, 2015–2022. (c) Gellman, S. H. *Acc. Chem. Res.* **1998**, *31*, 173–180. (d) Kirschenbaum, K.; Zuckerman, R. N.; Dill, D. A. *Curr. Opin. Struct. Biol.* **1999**, *9*, 530–535. (e) Stigers, K. D.; Soth, M. J.; Nowick, J. S. *Curr. Opin. Chem. Biol.* **1999**, *3*, 714–723. (f) Smith, M. D.; Fleet, G. W. J. *J. Pept. Sci.* **1999**, *5*, 425–441. (g) Cheng, R. P.; Gellman, S. H.; De Grado, W. F. *Chem. Rev.* **2001**, *101*, 3219–3232. (h) Venkatraman, J.; Shankaramma, S. C.; Balaram, P. *Chem. Rev.* **2001**, *101*, 3131–3152. (i) Cubberley, M. S.; Iverson, B. L. *Curr. Opin. Chem. Biol.* **2001**, *5*, 650–653. (j) Martinek, T. A.; Fülöp, F. *Eur. J. Biochem.* **2003**, *270*, 3657–3666. (k) Seebach, D.; Beck, A. K.; Bierbaum, D. J. *Chem. Biodiversity* **2004**, *1*, 1111–1239. (l) Goodman, C. M.; Choi, S.; Shandler, S.; DeGrado, W. F. *Nature Chem. Biol.* **2007**, *3*, 252–262. (m) Hecht, S.; Huc, I., Eds. *Foldamers: Structure, Properties and Applications*; Wiley-VCH: Weinheim, Germany, 2007.

and proteins¹ and opens up considerable possibilities for a rational peptide design and mimicry. This development began with the investigation of β -peptides^{1a–c,j,k} more than 10 years ago and was continued with the oligomers of the higher homologous γ - and δ -amino acids.^{1a,j,k,2} Important stimulation came from the suggestion to employ dipeptide repeats of various homologous amino

(2) (a) Brenner, M.; Seebach, D. *Helv. Chim. Acta* **2001**, *84*, 1181–1189. (b) Hintermann, T.; Gademann, K.; Jaun, B.; Seebach, D. *Helv. Chim. Acta* **1998**, *81*, 983–1002. (c) Hanessian, S.; Luo, X. H.; Schaum, R.; Michnick, S. *J. Am. Chem. Soc.* **1998**, *120*, 8569–8570. (d) Hanessian, S.; Luo, X. H.; Schaum, R. *Tetrahedron Lett.* **1999**, *40*, 4925–4929. (e) Vasudev, P. G.; Shamala, N.; Ananda, K.; Balaram, P. *Angew. Chem., Int. Ed.* **2005**, *44*, 4972–4975. (f) Grison, C.; Coutrot, P.; Geneve, C.; Didierjean, C.; Marraud, M. *J. Org. Chem.* **2005**, *70*, 10753–10764. (g) Szabo, L.; Smith, B. L.; McReynolds, K. D.; Parrill, A. L.; Morris, E. R.; Gervay, J. *J. Org. Chem.* **1998**, *63*, 1074–1078.

acids.³ Indeed, α/β -hybrid peptides containing α - and β -amino acid constituents in 1:1 backbone alternation displayed a variety of helical structures⁴ and some of these peptides elicited substantial biological activity.⁵ In the meantime, this concept was successfully extended to α/γ -, α/δ -, and β/γ -hybrid peptides.⁶ In all these hybrid peptide classes, mixed or β -helices play an important role.⁷ Thus, 11/9-helices with alternating 11- and 9-membered hydrogen-bonded pseudocycles showing an alternate direction change of the hydrogen bonds along the sequence were found in α/β -hybrid peptides together with unidirectional 11-, 14/15-, and 12/13-helices.⁴ For α/γ - and α/δ -hybrid peptides, mixed 12/10-^{6a-c} and 13/11-helices^{6f} have been obtained, which are the counterparts of the 11/9-helices of α/β -hybrid peptides.^{4d,e} Structural investigations in these hybrid peptides provide a good example of the strength of combining theoretical and experimental studies. For some of the helices, theoretical prediction of most stable structures preceded the synthesis and other experiments.^{6b}

In this study, we extend the concept of hybrid peptides with dipeptide repeats and synthesized the first representatives of ordered structures in α/ε -hybrid peptides following a concerted strategy of theoretical and experimental methods as in our recent work on α/δ -hybrid peptides.^{6f} For this purpose, a new (*S*)-C-linked carbo- ε -amino acid [(*S*)- ε -Caa_(x)] was synthesized and combined with L-Ala in 1:1 alternation. It was interesting to find that progressive lengthening of the amino acid backbone up to ε -amino acids still allowed the formation of ordered secondary structures.

Results and Discussion

Theoretical Studies. A look at a sequence of α/ε -hybrid peptides with dimer periodicity (Figure 1) provides the folding patterns with hydrogen-bonded pseudocycles of different sizes given in Table 1. Various helix types belong to groups with unidirectional hydrogen bonds formed in forward or backward direction of the sequence (Figure 1a), respectively, or to mixed or β -helices, where the hydrogen bonds are alternately formed in forward and backward direction (Figure 1b). To find all formal possibilities of periodic folding patterns, a systematic conformational search was performed on blocked α/ε -hybrid peptide octamers following strategies already employed for other peptide foldamers.^{4d,6b,7c,8b,d,e} To avoid any restriction of the conformational space, side chains were omitted. The complete catalogue of all periodic backbone folding alternatives and their stability relationships obtained from this search opens up the possibility to look for substitution patterns which are suited to favor special helix types.

For our α/ε -hybrid peptide model, a pool of 10 485 750 conformations, was generated by a systematic variation of the backbone torsion angles (φ, ψ) of the α - and ($\varphi, \theta, \zeta, \rho, \mu, \psi$) of the ε -amino acid constituents in intervals of 45° considering the dipeptide periodicity (Figure 1). On the basis of general geometry criteria for hydrogen bonds, all conformations corresponding to the described hydrogen bonding patterns were selected (Table 1, Figure 1). A total of 192 conformations resulted from this procedure, which were starting points for complete geometry optimizations at the HF/6-31G* level of ab initio MO theory. Correlation effects on the structure were estimated by reoptimization of the HF/6-31G* conformers at the B3LYP/6-31G* level of density functional theory (DFT). These approximation levels have proved to be reliable enough to describe the possibilities of helix formation in peptide foldamers.^{8,9} The minimum character of all structures was confirmed by vibration analysis, which was also the basis for the estimation of the free enthalpy differences. To estimate the solvent influence,

(3) (a) Hagihara, M.; Anthony, N. J.; Stout, T. J.; Clardy, J.; Schreiber, S. L. *J. Am. Chem. Soc.* **1992**, *114*, 6568–6570. (b) Lokey, R. S.; Iverson, B. L. *Nature* **1995**, *375*, 303–305. (c) Huck, B. R.; Fisk, J. D.; Gellman, S. H. *Org. Lett.* **2000**, *2*, 2607–2610. (d) Nowick, J. S.; Powell, N. A.; Martinez, E. J.; Smith, E. M.; Noronha, G. J. *Org. Chem.* **1995**, *60*, 3763–3765. (e) Chatterjee, S.; Roy, R. S.; Balaram, P. *J. R. Soc., Interface* **2007**, *4*, 587–606. (f) Rai, R.; Vasudev, P. G.; Ananda, K.; Ragothama, S.; Shamala, N.; Karle, I. L.; Balaram, P. *Chem.–Eur. J.* **2007**, *13*, 5917–5926. (g) Sengupta, A.; Aravinda, S.; Shamala, N.; Raja, K.; Muruga, P.; Balaram, P. *Org. Biomol. Chem.* **2006**, *4*, 4214–4222. (h) Ananda, K.; Vasudev, P. G.; Sengupta, A.; Raja, K. M. P.; Shamala, N.; Balaram, P. *J. Am. Chem. Soc.* **2005**, *127*, 16668–16674. (i) Roy, R. S.; Balaram, P. *J. Pept. Res.* **2004**, *63*, 279–289. (j) Aravinda, S.; Ananda, K.; Shamala, N.; Balaram, P. *Chem.–Eur. J.* **2003**, *9*, 4789–4795. (k) Roy, R. S.; Karle, I. L.; Ragothama, S.; Balaram, P. *Proc. Natl. Acad. Sci. U.S.A.* **2004**, *101*, 16478–16482. (l) Banerjee, A.; Pramanik, A.; Bhattacharjya, S.; Balaram, P. *Biopolymers* **1996**, *39*, 769–777.

(4) (a) Hayen, A.; Schmitt, M. A.; Nagassa, N.; Thomson, K. A.; Gellman, S. H. *Angew. Chem., Int. Ed.* **2004**, *43*, 505–510. (b) De Pol, S.; Zorn, C.; Klein, C. D.; Zerbe, O.; Reiser, O. *Angew. Chem., Int. Ed.* **2004**, *43*, 511–514. (c) Seebach, D.; Jaun, B.; Sebesta, R.; Mathad, R. I.; Flögel, O.; Limbach, M.; Sellner, H.; Cottens, S. *Helv. Chim. Acta* **2006**, *89*, 1801–1825. (d) Baldauf, C.; Günther, R.; Hofmann, H.-J. *Biopolymers* **2006**, *84*, 408–413. (e) Sharma, G. V. M.; Nagendar, P.; Jayaprakash, P.; Krishna, P. R.; Ramakrishna, K. V. S.; Kunwar, A. C. *Angew. Chem., Int. Ed.* **2005**, *44*, 5878–5882. (f) Srinivasulu, G.; Kumar, S. K.; Sharma, G. V. M.; Kunwar, A. C. *J. Org. Chem.* **2006**, *71*, 8395–8400. (g) Choi, S. H.; Guzei, I. A.; Gellman, S. H. *J. Am. Chem. Soc.* **2008**, *129*, 13780–13781. (h) Choi, S. H.; Guzei, I. A.; Spencer, L. C.; Gellman, S. H. *J. Am. Chem. Soc.* **2008**, *130*, 6544–6550. (i) Prabhakaran, P.; Kale, S. S.; Puranik, V. G.; Rajamohanam, P. R.; Chetina, O.; Howard, J. A. K.; Hofmann, H.-J.; Sanjayan, G. J. *J. Am. Chem. Soc.* **2008**, *130*, 17743–17754.

(5) (a) Schmitt, M. A.; Weisblum, B.; Gellman, S. H. *J. Am. Chem. Soc.* **2004**, *126*, 6848–6849. (b) Sadowsky, J. D.; Schmitt, M. A.; Lee, H. S.; Umezawa, N.; Wang, S.; Tomita, Y.; Gellman, S. H. *J. Am. Chem. Soc.* **2005**, *127*, 11966–11968. (c) Horne, W. S.; Price, J. L.; Keck, J. L.; Gellman, S. H. *J. Am. Chem. Soc.* **2007**, *129*, 4178–4180. (d) Price, J. L.; Horne, W. S.; Gellman, S. H. *J. Am. Chem. Soc.* **2007**, *129*, 6376–6377. (e) Seebach, D.; Gardiner, J. *Acc. Chem. Res.* **2008**, *41*, 1366–1375. (f) David, R.; Günther, R.; Baumann, L.; Lühmann, T.; Seebach, D.; Hofmann, H.-J.; Beck-Sickinger, A. G. *J. Am. Chem. Soc.* **2008**, *130*, 15311–15317.

(6) (a) Sharma, G. V. M.; Jadhav, V. B.; Ramakrishna, K. V. S.; Jayaprakash, P.; Narasimulu, K.; Subash, V.; Kunwar, A. C. *J. Am. Chem. Soc.* **2006**, *128*, 14657–14668. (b) Baldauf, C.; Günther, R.; Hofmann, H.-J. *J. Org. Chem.* **2006**, *71*, 1200–1208. (c) Chatterjee, S.; Vasudev, P. G.; Ragothama, S.; Shamala, N.; Balaram, P. *Biopolymers* **2008**, *90*, 759–771. (d) Vasudev, P. G.; Chatterjee, S.; Ananda, K.; Shamala, N.; Balaram, P. *Angew. Chem., Int. Ed.* **2008**, *47*, 6430–6432. (e) Vasudev, P. G.; Ananda, K.; Chatterjee, S.; Aravinda, S.; Shamala, N.; Balaram, P. *J. Am. Chem. Soc.* **2007**, *129*, 4039–4048. (f) Sharma, G. V. M.; Babu, B. S.; Ramakrishna, K. V. S.; Nagendar, P.; Kunwar, A. C.; Schramm, P.; Baldauf, C.; Hofmann, H.-J. *Chem.–Eur. J.* **2009**, *15*, 5552–5566. (g) Saludes, J. P.; Ames, J. B.; Gervay-Hague, J. *J. Am. Chem. Soc.* **2009**, *131*, 5495–5505.

(7) (a) Ramachandran, G. N.; Chandrasekaran, R. *Indian J. Biochem. Biophys.* **1972**, *9*, 1–4. (b) De Santis, P.; Morosetti, S.; Rizzo, R. *Macromolecules* **1974**, *7*, 52–58. (c) Baldauf, C.; Günther, R.; Hofmann, H.-J. *Angew. Chem., Int. Ed.* **2004**, *43*, 1594–1597.

(8) (a) Möhle, K.; Günther, R.; Thormann, M.; Sewald, N.; Hofmann, H.-J. *Biopolymers* **1999**, *50*, 167–184. (b) Baldauf, C.; Günther, R.; Hofmann, H.-J. *Helv. Chim. Acta* **2003**, *86*, 2573–2588. (c) Baldauf, C.; Günther, R.; Hofmann, H.-J. *Biopolymers* **2005**, *80*, 675–687. (d) Baldauf, C.; Günther, R.; Hofmann, H.-J. *J. Org. Chem.* **2004**, *69*, 6214–6220. (e) Baldauf, C.; Günther, R.; Hofmann, H.-J. *J. Org. Chem.* **2005**, *70*, 5351–5361. (f) Baldauf, C.; Günther, R.; Hofmann, H.-J. *Phys. Biol.* **2006**, *3*, S1–S9. (g) Günther, R.; Hofmann, H.-J. *Helv. Chim. Acta* **2002**, *85*, 2149–2168.

(9) (a) Wu, Y.-D.; Wang, D.-P. *J. Am. Chem. Soc.* **1998**, *120*, 13485–13493. (b) Wu, Y.-D.; Wang, D.-P. *J. Am. Chem. Soc.* **1999**, *121*, 9352–9362. (c) Beke, T.; Csizmadia, I. G.; Perczel, A. *J. Comput. Chem.* **2004**, *25*, 285–307. (d) Beke, T.; Csizmadia, I. G.; Perczel, A. *J. Am. Chem. Soc.* **2006**, *128*, 5158–5167. (e) Wu, Y.-D.; Han, W.; Wang, D.-P.; Gao, Y.; Zhao, Y.-L. *Acc. Chem. Res.* **2008**, *41*, 1418–1427.

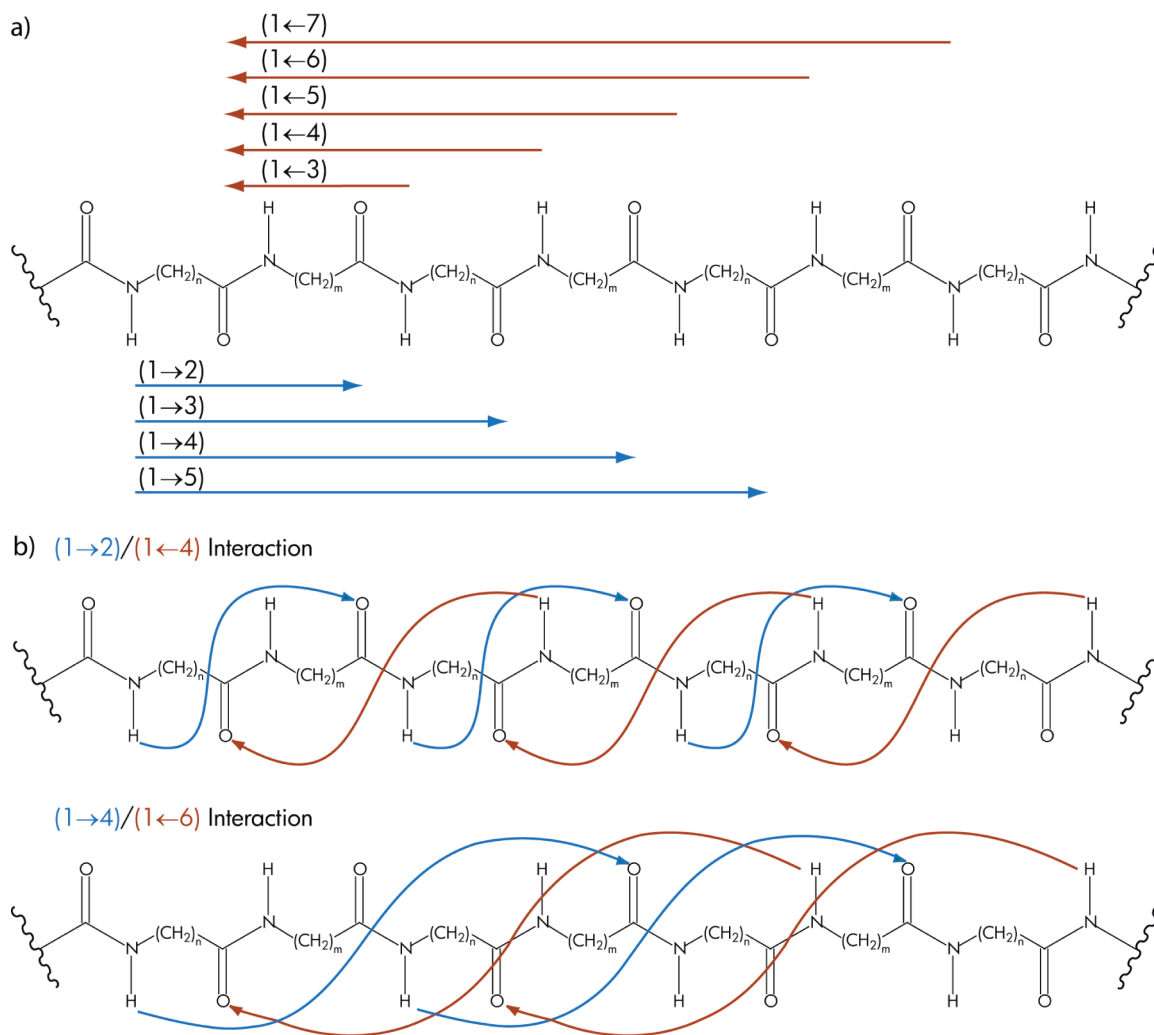


FIGURE 1. Possible hydrogen bonding patterns for helices of α/ϵ -hybrid peptides: (a) with unidirectional hydrogen bonds either in forward or in backward directions of the sequence; (b) with hydrogen bonds alternately changing their directions ($n/m = 1$: α -amino acid; $n/m = 5$: ϵ -amino acid).

TABLE 1. Formal Possibilities of Hydrogen-Bonded Helices in α/ϵ -Hybrid Peptides

relative positions of interacting amino acids ^a	type of interacting amino acids ^{a,b}	alternating pseudocycles C_x/C_y ^c	helix notation	no. of representatives
1→2/1←4	$\alpha \rightarrow \epsilon / \alpha \leftarrow \epsilon$	C_{12}/C_{14}	$H_{12/14}$	8
	$\epsilon \rightarrow \alpha / \epsilon \leftarrow \alpha$	C_{14}/C_{12}	$H_{14/12}$	6
1→4/1←6	$\alpha \rightarrow \epsilon / \alpha \leftarrow \epsilon$	C_{22}/C_{24}	$H_{22/24}$	7
	$\epsilon \rightarrow \alpha / \epsilon \leftarrow \alpha$	C_{24}/C_{22}	$H_{24/22}$	9
1→2	$\alpha \rightarrow \epsilon / \epsilon \rightarrow \alpha$	C_{12}/C_{12}	H_{12}	6
1→3	$\alpha \rightarrow \alpha / \epsilon \rightarrow \epsilon$	C_{15}/C_{19}	$H_{15/19}$	4
1→4	$\alpha \rightarrow \epsilon / \alpha \rightarrow \epsilon$	C_{22}/C_{22}	H_{22}	3
1←3	$\alpha \leftarrow \alpha / \epsilon \leftarrow \epsilon$	C_7/C_{11}	$H_{7/11}$	6
1←4	$\alpha \leftarrow \epsilon / \epsilon \leftarrow \alpha$	C_{14}/C_{14}	H_{14}	6
1←5	$\alpha \leftarrow \alpha / \epsilon \leftarrow \epsilon$	C_{17}/C_{21}	$H_{17/21}$	0
1←6	$\alpha \leftarrow \epsilon / \epsilon \leftarrow \alpha$	C_{24}/C_{24}	H_{24}	0

^a→: forward direction. ←: backward direction of the hydrogen bonds. ^b α : α -amino acid. ϵ : ϵ -amino acid. ^c x, y : number of atoms in alternating hydrogen-bonded pseudocycles.

single-point calculations on the HF/6-31G* conformers were performed for an aqueous environment employing a polarizable continuum model (IEFPCM).

The conformational search provided 55 helical conformers. Their distribution on the various helix types is given in the last column of Table 1. In Table 2, the relative energies of

the most stable helical conformer of each helix pattern are summarized. Table 3 shows the HF/6-31G* backbone torsion angles. The corresponding data for all other helix conformers at all approximation levels are given in the Supporting Information. In Figure 2, representative examples of the various helix types are illustrated.

TABLE 2. Relative Energies^a and Free Enthalpies^a of the Most Stable Helices of Alternating α/ϵ -Hybrid Peptide Octamers in Vacuo (HF/6-31G*, B3LYP/6-31G*) and in an Aqueous Environment (PCM//HF/6-31G*)

helix ^c	ΔE			ΔG^b
	HF/6-31G*	B3LYP/6-31G*	PCM//HF/6-31G* ^{d,e}	
H _{12/14} ^I	6.6	7.8	14.2	27.4
H _{14/12} ^I	3.0	0.0^f	11.1	12.4
H _{22/24} ^I	0.0^g	1.6	9.8	13.6
H _{24/22} ^I	9.1	11.4	8.9	0.0^h
H ₁₂ ^I	74.1	73.1	13.1	71.7
H _{15/19} ^I	87.3	96.1	24.8	88.6
H ₂₂ ^I	124.0	138.3	37.3	105.3
H _{7/11} ^I	55.6	54.8	50.5	68.8
H ₁₄ ^I	55.5	67.9	2.5	63.0

^a In kJ/mol. ^b HF/6-31G*. ^c See Table 1. ^d $\epsilon = 78.4$. ^e Helix H₁₄^I is most stable at this approximation level with $E_T = -2526.106196$ au and, therefore, reference point for this column; $\Delta E_T(\text{HF}/6-31\text{G}^*)$ for H₁₄^I = 67.7 kJ/mol; $\Delta E_T(\text{B3LYP}/6-31\text{G}^*)$ for H₁₄^I = 66.7 kJ/mol. ^f $E_T = -2541.7010474$ au. ^g $E_T = -2526.1416676$ au. ^h $G = -2525.155819$ au.

Most stable are the mixed helices H_{14/12}^I, H_{22/24}^I, H_{12/14}^I, and H_{24/22}^I. Their energies are close together at all approximation levels. Following our convention with α/γ - and β/γ -hybrid peptides,^{6a,b} a mixed 12/14-helix results, when the amide protons of the α -residues take part in the hydrogen bonding of 12-membered rings and those of the ϵ -residues in the formation of 14-membered rings. The reverse situation leads to a 14/12-helix (Figure 1). H_{14/12}^I is most stable in vacuum considering correlation energy, whereas H_{22/24}^I is slightly favored at the Hartree–Fock level.

Mixed or β -helices are generally disadvantaged in more polar environments in comparison to helix types with unidirectional hydrogen bonds due to their smaller macrodipole moments resulting from the alternate change of the hydrogen bond directions.^{4d,6b,7c,8a,c} Indeed, the two helices H₁₄^I and H₁₄^I with backward directions of the hydrogen bonds are predicted to be slightly more stable than the most stable mixed helices (Table 2).

Peptide Syntheses. The peptides **2–5** (Figure 3) were prepared by the standard peptide coupling method, using EDCI,¹⁰ HOBt, and DIPEA in solution phase. The constituent monomers, (S)- ϵ -Caa(_x) and L-Ala, were obtained from the corresponding Boc-(S)- ϵ -Caa(_x)-OMe (**1**) and Boc-L-Ala-OMe (**A**), respectively. The requisite **1** (see the Supporting Information)¹¹ was prepared from the known Boc-(S)- δ -Caa-OMe^{6f} by the homologation method. The synthesis of the peptides **2–5** is outlined in Scheme 1. Accordingly, treatment of **1** with CF₃COOH in CH₂Cl₂ at room temperature for 2 h afforded the TFA salt **6**. Similarly, ester **1** on hydrolysis with aq 4 N NaOH at room temperature for 2 h gave the corresponding acid **7** in 94% yield. Peptide coupling of the salt **6** with acid **8** in the presence of EDCI, HOBt, and DIPEA in CH₂Cl₂ at room temperature for 4 h afforded the dipeptide **10** in 84% yield. Likewise, acid **7** on coupling with salt **9** in the presence of EDCI, HOBt, and DIPEA in CH₂Cl₂ gave the dipeptide **11** in 90% yield. Acid (CF₃COOH) mediated hydrolysis of the Boc group in **11** at room temperature furnished the salt **12**, which on further coupling (EDCI, HOBt, and DIPEA) with **8** in CH₂Cl₂ at room temperature

for 4 h gave the tripeptide **2** in 82% yield. Base (aq 4 N NaOH) hydrolysis of **2** gave the acid **13**, which on coupling with **12** under the above reaction conditions at room temperature for 4 h afforded the pentapeptide **4** in 56% yield. Peptide **10** on hydrolysis with aq 4 N NaOH gave the acid **14**, while **10** on exposure to CF₃COOH furnished the salt **15**. Peptide coupling of **14** in the presence of EDCI, HOBt, and DIPEA with **15** at room temperature for 4 h in CH₂Cl₂ afforded the tetrapeptide **3** in 46% yield. Furthermore, peptide **3** on base (aq 4 N NaOH) hydrolysis gave the acid **16**, which on coupling with the salt **15** in the presence of EDCI, HOBt, and DIPEA in CH₂Cl₂ provided the hexapeptide **5** in 46% yield.

Conformational Analysis. The proton NMR spectra of peptides **2** and **3** did not show signatures of any secondary structure. In the ¹H NMR spectrum of peptide **4**,¹¹ four amide protons, NH(2) to NH(5), displayed downfield shifts ($\delta_{\text{NH}} > 7$ ppm), suggesting their involvement in hydrogen bonding. Solvent titration studies (see the Supporting Information) showed very small chemical shift changes ($\Delta\delta_{\text{NH}} < 0.40$ ppm) for NH(2) to NH(5), thus confirming their participation in hydrogen bonding. For the Boc-urethane NH, the $\Delta\delta_{\text{NH}} > 1.0$ ppm clearly indicates its nonparticipation in H-bonding. For the ϵ -residue, $^3J_{\text{NH}-\text{C}_\epsilon\text{H}} = 9.7$ Hz is consistent with an antiperiplanar arrangement of NH and C _{ϵ} H, corresponding to a value of $\sim 120^\circ$ for the torsion angle $\varphi(\epsilon)$ (C(O)–N–C _{ϵ} –C _{δ}). One very strong and another rather weak NOE correlation between the amide protons of the third and fifth residues [NH(3) and NH(5)] with both the C _{α} H of the preceding ϵ -residue, NH(3)/C _{α} H(2) and NH(5)/C _{α} H(4) (for convenience we denote the C _{α} H as the one with the weaker and C _{α'} H as the one with the stronger NOE cross peaks), support a value of $\pm 120^\circ$ for $\psi(\epsilon)$ (C _{β} –C _{α} –C(O)–N). NH(2)/C _{δ} H(2), NH(4)/C _{δ} H(4), and C _{δ} H(4)/C _{α} H(4) NOE correlations provide strong evidence for the backbone torsion angles $\theta(\text{N}-\text{C}_\epsilon-\text{C}_\delta-\text{C}_\gamma)$ being constrained. The presence of medium range NOE, C _{α} H-(2)/C _{γ} H(2), along with a rather strong NOE C _{β} H(4)/C _{δ} H(4) suggest constrained values of the intervening dihedral angles θ , ζ (C _{ϵ} –C _{δ} –C _{γ} –C _{β}), ρ (C _{δ} –C _{γ} –C _{β} –C _{α}), and μ (C _{γ} –C _{β} –C _{α} –C(O)). $^3J_{\text{C}_\alpha\text{H}-\text{C}_\beta\text{H}} = 4.3$ Hz and $^3J_{\text{C}_\alpha\text{H}-\text{C}_\beta\text{H}} = 10.2$ Hz for the second residue, and $^3J_{\text{C}_\alpha\text{H}-\text{C}_\beta\text{H}}$ and $^3J_{\text{C}_\alpha\text{H}-\text{C}_\beta\text{H}} \approx 5.0$ Hz for the fourth residue further support a constrained value of μ . For the α -residues, values of $^3J_{\text{NH}-\text{C}_\alpha\text{H}} \approx 7$ Hz are not distinctive and do not permit distinction between likely averaging over several conformations or a single well-defined value for $\psi(\alpha)$. However, strong NH(2)/C _{α} H(1) NOE correlation is consistent with $\psi(\alpha) \approx 120^\circ$ for the N-terminal α -residue.

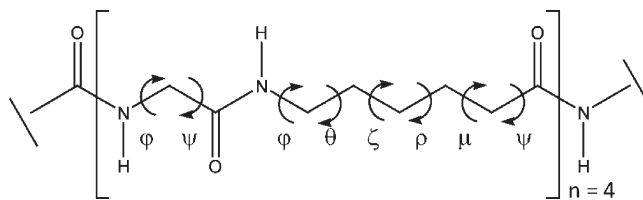
Due to spectral overlaps it was not possible to get individual chemical shifts for several protons. Similarly, most of the coupling constants involving C _{β} -, C _{γ} -, and C _{δ} -protons of ϵ -residues prevented us from deducing more definitive values of θ , ζ , ρ , and μ . The NOE correlations C _{α} H(1)/NH(3) and C _{α} H(3)/NH(5) are reminiscent of very distinctive features in all our mixed helices, where the amide proton of the i th residue is in the proximity to the backbone protons of the ($i-2$)th residue due to a hydrogen bond between NH(i) and CO($i-3$). In this case, such a hydrogen bond forms a 14-membered pseudocycle.

Molecular dynamics (MD) calculations for **4**¹¹ were carried out by using the distance constraints derived from the ROESY experiments, using two-spin approximation. The 15 lowest energy structures obtained have a backbone rmsd of 0.51 Å and a heavy atoms rmsd of 0.63 Å. The average value

(10) (a) Chan, L. C.; Cox, G. B. *J. Org. Chem.* **2007**, *72*, 8863–8869.

(b) Bodanszky, M. *Peptide Chemistry: A Practical Textbook*; Springer: New York, 1988.

(11) See the Supporting Information.

TABLE 3. Backbone Torsion Angles^a of the Most Stable Helices of Alternating α/ϵ -Hybrid Peptide Octamers at the HF/6-31G* Level of ab Initio MO Theory

helix ^b	ϕ	θ	ζ	ρ	μ	ψ
H _{12/14} ^I	87.1					-70.5
	-105.7	55.4	67.7	-172.4	78.0	102.8
	135.5					-64.2
	-113.0	54.8	65.9	-169.7	78.5	105.2
	135.9					-67.1
H _{14/12} ^I	-113.5	55.5	66.6	-169.9	78.8	104.6
	136.4					-73.4
	-109.1	55.6	66.6	-170.4	76.0	98.3
	-78.6					151.8
	104.6	-73.9	158.1	-88.4	75.3	-127.9
H _{22/24} ^I	-79.0					143.5
	110.3	-72.8	159.2	-88.6	74.5	-124.3
	-79.1					143.6
	109.9	-72.6	160.2	-89.6	73.5	-122.5
	-76.5					138.1
H _{24/22} ^I	111.2	-69.7	165.3	-90.4	68.5	-118.0
	85.3					-77.7
	-82.3	-180.0	-176.6	179.8	-178.9	118.0
	84.5					-76.6
	-88.6	-177.3	-178.2	-179.1	-178.8	104.2
H ₁₂ ^I	108.2					-103.1
	-82.7	-175.6	-176.2	-176.9	-176.2	98.7
	120.8					-128.9
	-77.4	179.3	-177.0	-179.9	179.9	117.0
	-141.7					158.1
H _{15/19} ^I	106.4	-70.1	162.4	177.4	167.1	-151.5
	-124.3					143.3
	99.8	-67.6	168.7	-179.0	164.7	168.3
	-74.7					117.4
	111.0	-66.7	177.1	179.0	170.4	173.6
H ₂₂ ^I	-77.2					102.5
	122.6	-66.8	177.4	178.7	179.3	-166.6
	95.6					151.1
	129.0	-45.1	-56.2	170.1	-67.5	110.3
	101.1					135.4
H _{7/11} ^I	141.3	-45.9	-54.5	167.6	-68.4	111.1
	98.2					138.8
	138.9	-45.1	-54.4	168.1	-68.5	111.1
	97.9					143.6
	121.0	-50.2	-57.6	179.8	-68.2	159.7
H ₁₄ ^I	100.1					144.1
	97.1	-62.9	-175.7	180.0	70.6	20.9
	98.0					158.4
	101.9	-66.7	176.1	176.0	61.5	47.8
	103.3					144.5
H ₂₂ ^I	101.6	-67.5	179.3	177.9	59.9	56.0
	99.2					146.7
	98.3	-76.6	-178.5	170.4	63.7	85.7
	98.7					143.1
	75.4	176.7	174.7	175.4	174.2	86.8
H _{15/19} ^I	93.1					76.1
	83.3	179.6	-176.1	-179.9	-176.2	98.9
	92.1					61.9
	89.9	179.7	-171.7	-178.7	-170.9	97.8
	87.1					87.8
H _{7/11} ^I	77.5	-176.7	176.4	-177.7	175.9	145.2
	85.8					-50.4
	78.3	-151.2	70.2	69.0	-166.8	90.3
	85.0					-52.4
	81.0	-146.9	68.7	65.7	-173.2	84.2
H ₁₄ ^I	83.5					-53.9
	85.6	-162.0	59.3	58.9	-162.2	108.1
	85.5					-58.0
	83.4	-168.1	53.8	56.4	-158.4	92.8
	-73.9					-34.6
H ₁₄ ^I	-123.7	50.8	53.6	-174.5	156.8	-84.9
	-73.2					-36.2
	-122.1	50.0	54.2	-173.3	156.8	-86.4
	-73.8					-34.9
	-122.0	49.8	53.7	-173.8	157.2	-85.5
H ₁₄ ^I	-78.2					-27.3
	-137.0	48.8	52.6	-177.7	169.6	-89.1

^aIn degrees. ^bSee Table 1.

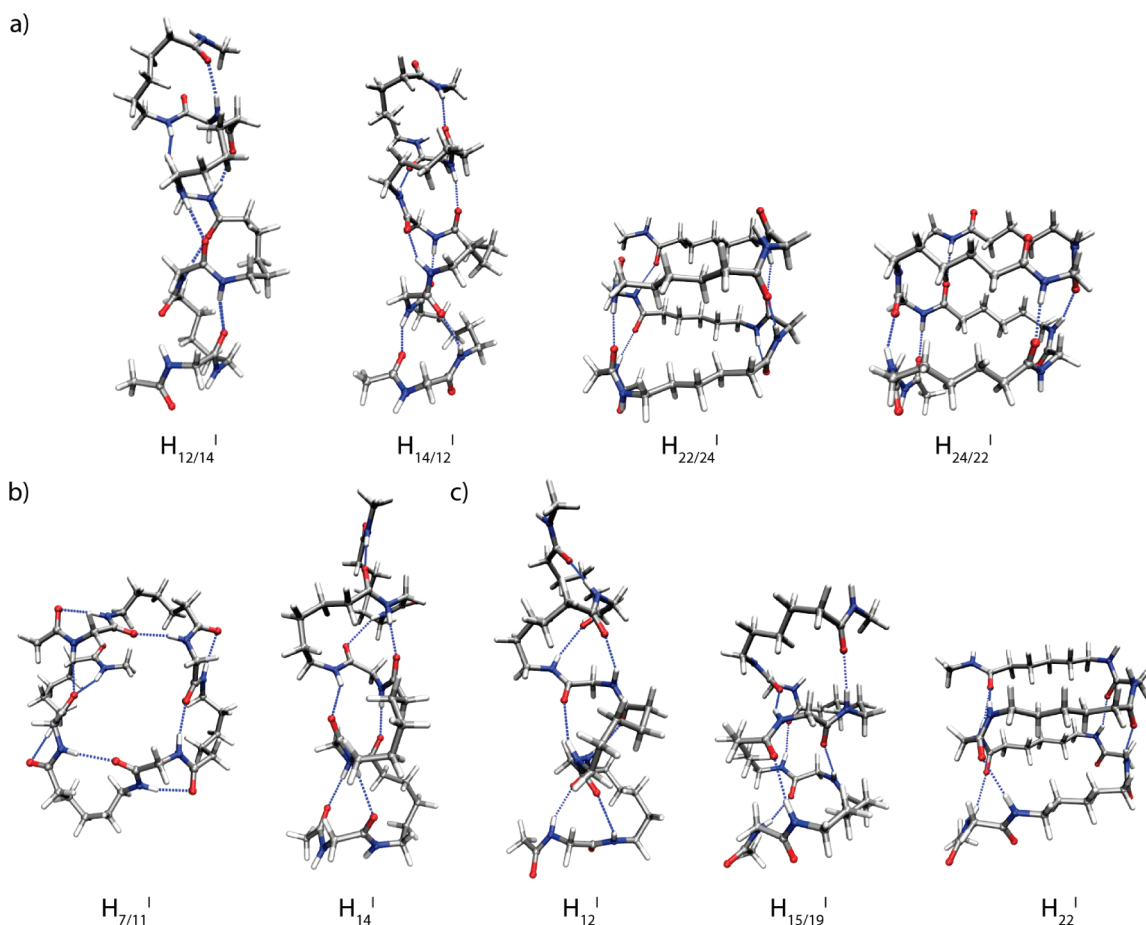
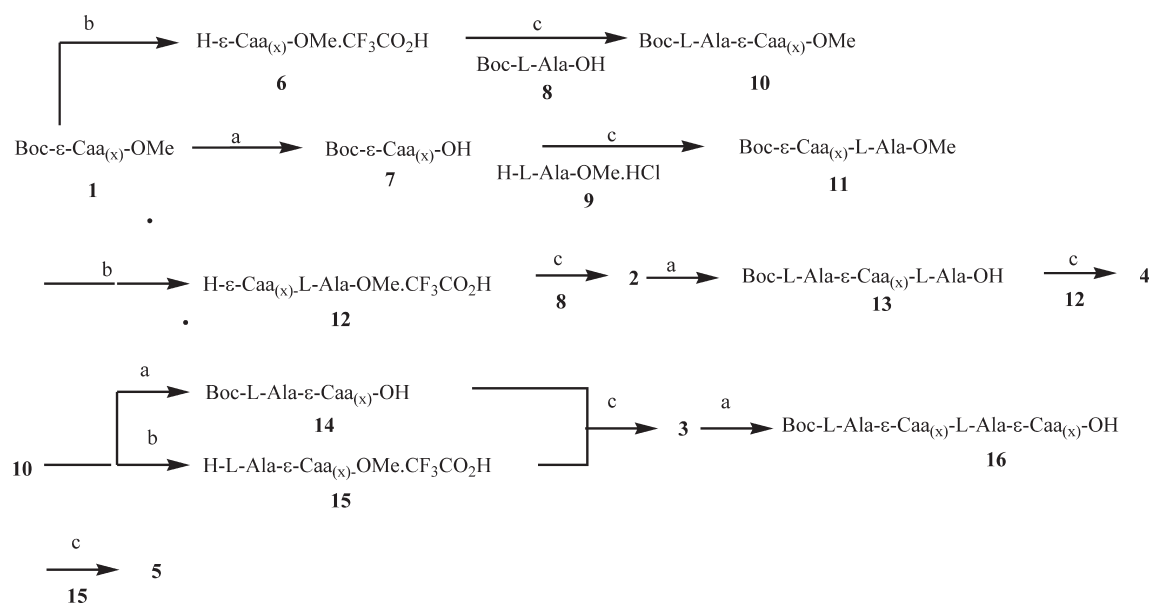


FIGURE 2. Most stable helix types for various hydrogen bond patterns of α/ϵ -hybrid peptides: (a) mixed helices; (b) helices with backward hydrogen bond directions; and (c) helices with forward hydrogen bond directions.

SCHEME 1. Synthesis of Peptides 2–5



Reagents and conditions: (a) aq 4 N NaOH, MeOH, 0 °C–rt, 2 h; (b) CF₃COOH, dry CH₂Cl₂, 2 h; (c) HOBt (1.2 equiv), EDCI (1.2 equiv), DIPEA (1.5 equiv), dry CH₂Cl₂, 0 °C–rt, 4 h.

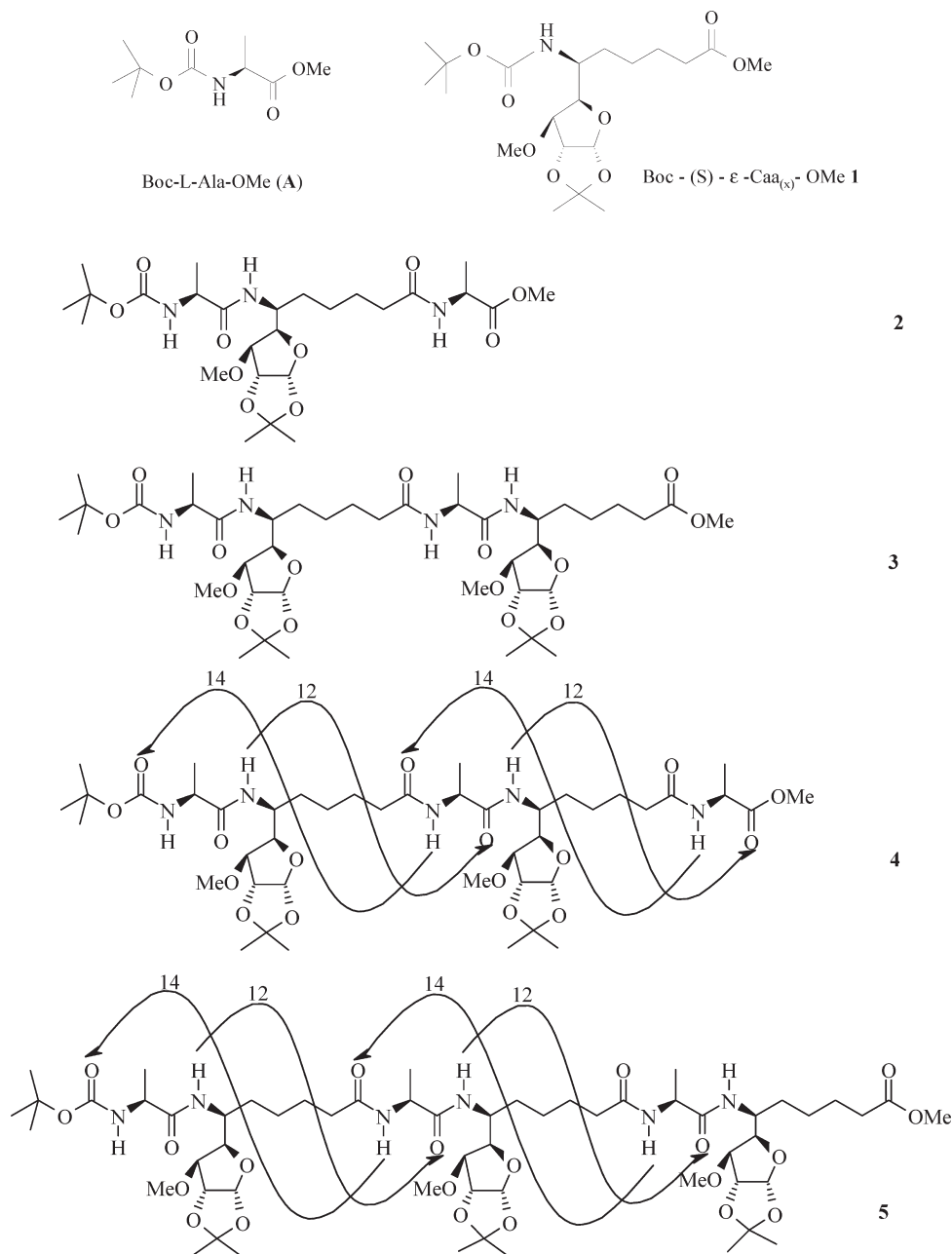


FIGURE 3. Structures of peptides **2** to **5** (arrows indicate the hydrogen bonding pattern).

of the dihedral angles for **4**, obtained after removing the terminal residues (in order to reduce the effect of the fraying), are $\varphi(\alpha) = (-79 \pm 2)^\circ$, $\psi(\alpha) = (111 \pm 12)^\circ$ and $\varphi(\epsilon) = (119 \pm 5)^\circ$, $\theta = (-70 \pm 3)^\circ$, $\zeta = (170 \pm 3)^\circ$, $\rho = (-90 \pm 3)^\circ$, $\mu = (72 \pm 4)^\circ$, and $\psi(\epsilon) = (-102 \pm 3)^\circ$ for the two amino acid constituents. These values agree fairly well with the theoretically estimated average backbone torsion angles for the $H_{14/12}^1$ -helix of **4**, which are $\varphi(\alpha) = -75.3^\circ$, $\psi(\alpha) = 144.9^\circ$ and $\varphi(\epsilon) = 117.7^\circ$, $\theta = -72.0^\circ$, $\zeta = 154.8^\circ$, $\rho = -85.6^\circ$, $\mu = 77.2^\circ$, and $\psi(\epsilon) = -131.8^\circ$.

The ^1H NMR spectrum of **5** showed that four of the amide protons (except the N- and C-terminal ones) appear at $\delta_{\text{NH}} > 7$ ppm, which suggests their participation in hydrogen bonding. Further confirmation for this was derived from

solvent titration studies with $\Delta\delta_{\text{NH}} < 0.29$ ppm for $\text{NH}(2)$ to $\text{NH}(5)$ (Figure 4). For the ϵ - residues, the coupling constant $^3J_{\text{NH}-\text{C}_\alpha\text{H}} > 9.0$ Hz suggests an antiperiplanar arrangement of NH and C_αH , which is consistent with a value of $\sim 120^\circ$ for the torsion angle $\varphi(\epsilon)$. Due to spectral overlap only little information could be obtained, yet it was heartening to find $^3J_{\text{C}_\alpha\text{H}-\text{C}_\beta\text{H}}$ values of 3.9 and 9.5 Hz for the 6th residue, and, as for **4**, a very strong $\text{NH}(4)/\text{C}_\beta\text{H}(4)$ NOE cross peak giving support for a constrained value for $\theta \approx \pm 60^\circ$. As in **4**, one strong and another rather weak NOE correlation involving $\text{NH}(3)$ and $\text{C}_\alpha\text{H}(2)$ and also $\text{NH}(5)$ and $\text{C}_\alpha\text{H}(4)$ provide adequate evidence for a value of $\pm 120^\circ$ for $\psi(\epsilon)$. The presence of very strong $\text{C}_\alpha\text{H}(2)/\text{C}_\gamma\text{H}(2)$ and $\text{C}_\alpha\text{H}(4)/\text{C}_\gamma\text{H}(4)$ correlations (C_αH being the

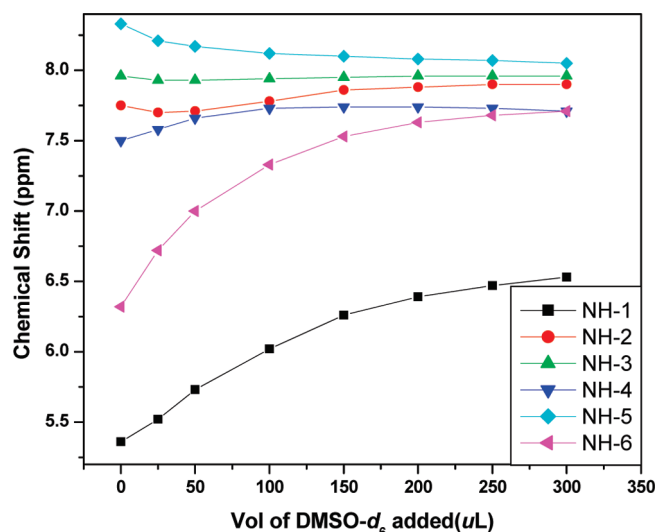


FIGURE 4. Solvent titration plot for peptide 5.

proton in the ϵ -residue with a strong NOE correlation to the NH of the following residue) as well as $C_{\beta}H(4)/C_{\delta}H(4)$ NOEs suggested constrained values of the intervening dihedral angles θ , ζ , ρ , and μ (Figure 5). Further support for this comes from medium range NOEs NH(2)/ $C_{\delta}H(2)$, NH(4)/ $C_{\delta}H(4)$, C4H(2)/ $C_{\delta}H(2)$, and C4H(4)/ $C_{\delta}H(4)$. As in 4 for the α -residue, values of ${}^3J_{NH-C_{\alpha}H} \approx 7$ Hz are not distinctive, yet strong NH(2)/ $C_{\alpha}H(1)$ NOE correlation supports $\psi(\alpha) \approx 120^\circ$ for the N-terminal α -residue. The distinctive signature of a 14/12-helix was observed in the ROESY spectrum (Figure 6), in which the NOE correlations for NH(3)/ $C_{\alpha}H(1)$ and NH(5)/ $C_{\alpha}H(3)$ support 14-membered hydrogen bonds for Boc-C=O \cdots H-N(3) and (2)C=O \cdots H-N(5), respectively. Similarly, the presence of weak, but characteristic NOEs NH(2)/NH(3) and NH(4)/NH(5) is characteristic with 12-membered hydrogen bonds between (2)N-H \cdots O=C (3) and (4)N-H \cdots O=C (5), respectively.

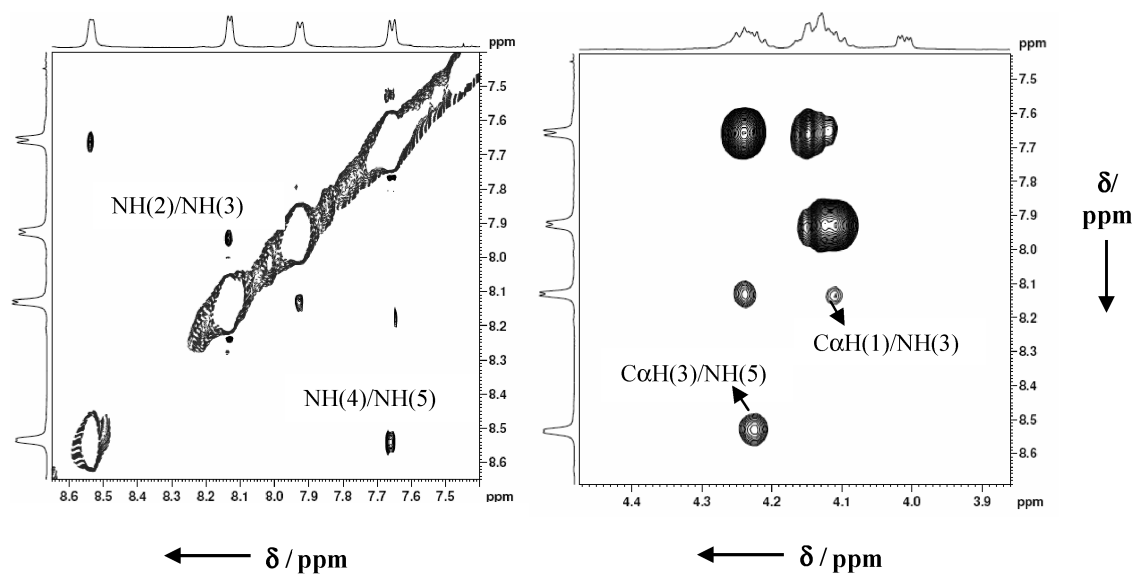


FIGURE 6. Fingerprint region in the ROESY spectrum of peptide 5.

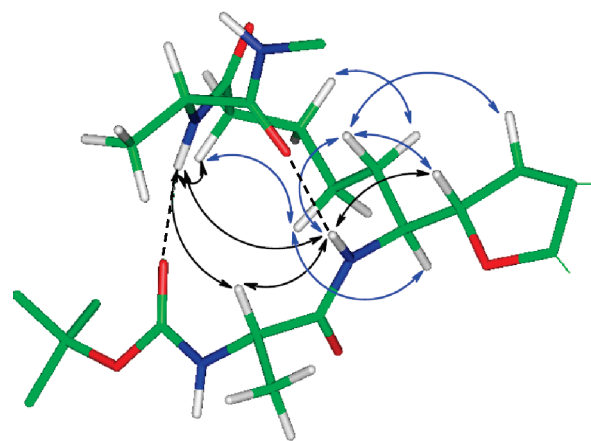


FIGURE 5. Characteristic NOEs supporting 14- and 12-membered hydrogen bonding (structure determination on the basis of the NMR measurements in $CDCl_3$ solution). Dark arrows represent NOEs, which are unique. The NOEs represented by blue double arrows are ambiguous (stereospecific assignment of the protons at C_{α} , C_{β} , C_{γ} , and C_{δ} could not be made). These are thus the NOEs observed and correspond to those expected from the helix model derived from the theoretical calculations. Dotted lines represent the H-bonds.

In Figure 7, the superimposition of the 15 lowest energy structures obtained from MD calculations on 5 having a backbone rmsd of 0.94 Å and a heavy atom rmsd of 1.01 Å is shown.¹¹ To reduce the effect of fraying, the average values of the dihedral angles for 5 were obtained by removing the terminal residues. They are $\varphi(\alpha) = (-75 \pm 3)^\circ$, $\psi(\alpha) = (123 \pm 5)^\circ$, and $\varphi(\epsilon) = (101 \pm 2)^\circ$, $\theta = (-75 \pm 1)^\circ$, $\zeta = (173 \pm 1)^\circ$, $\rho = (-89 \pm 2)^\circ$, $\mu = (71 \pm 2)^\circ$, and $\psi(\epsilon) = (-111 \pm 3)^\circ$ for the two amino acid constituents.

The CD spectra¹¹ of a 0.2 mM solution in methanol for both 4 and 5 show a narrow negative maxima at ~ 194 nm and another broad shallow negative maxima at about 225–228 nm, while the $[\theta]$ values show a crossover point at around 205 nm. Though the molecular ellipticities $[\theta]$ per residue are rather small, the pentamer 4, with $[\theta] \approx 7000$ deg \cdot cm 2 .

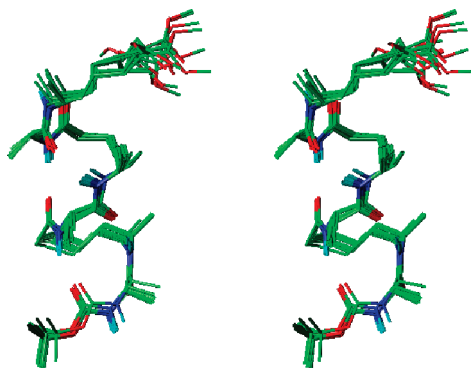


FIGURE 7. Stereoview of the superimposition of the 15 lowest energy structures for peptide **5** (for clarity, sugars are replaced with methyl groups after the calculations).

dmol^{-1} , has stronger differential absorption than the larger hexamer **5**, with $[\theta] \approx 5000$, suggesting a more robust secondary structure for **4**.

Conclusions

Stimulated by a systematic theoretical conformational analysis based on ab initio MO theory, the novel foldamer class of α/ϵ -hybrid peptides is presented in this study. The detailed NMR structure analyses show the formation of a novel 14/12-motif. This mixed or β -helix was predicted to be most stable according to the theoretical calculations. Despite the high flexibility of the backbone, which is expected in the ϵ -amino acid constituents, the formation of stable ordered secondary structures is still possible in this hybrid peptide class. The pool of theoretically predicted folding patterns may serve to find further secondary structure types by introduction of suited substituents in the backbone.

Experimental Section

NMR spectra (1D and 2D experiments) for peptides **2–5** were obtained at 200, 400, and 600 MHz (^1H), and at 100 and 150 MHz (^{13}C). Chemical shifts are reported in δ scale with respect to internal TMS reference. Information on hydrogen bonding in CDCl_3 was obtained from solvent titration studies at 298 K by sequentially adding up to 300 μL of $\text{DMSO-}d_6$ in 600 μL of CDCl_3 solution of peptides.

The CD spectra were obtained with a spectropolarimeter in rectangular fused quartz cells of 0.2 cm path length at room temperature with a scan range of 190–260 nm and scanning speed of 50 nm/min, using peptide concentrations of 0.2 mM in MeOH. The binomial method was used for smoothing the spectra. The values are expressed in terms of $[\theta]$, the total molar ellipticity ($\text{deg} \cdot \text{cm}^2 \cdot \text{dmol}^{-1}$)/residue.

The Insight-II program was used for construction of molecular model and for structural analysis of different obtained conformations. The DISCOVER software was used for molecular modeling calculations, including energy minimization. The CVFF MSI version with default parameter was used as the force field throughout the calculation, using a distance dependent dielectric constant with $\epsilon = 4.8$ (dielectric constant of deuterated chloroform). The constraints were derived from the volume integrals obtained from the ROESY spectra by using a two-spin approximation and a reference distance of 2.37 Å for the vicinal protons C1H and C2H in the sugar ring, which has

been shown by us to take a ^3_2T conformation earlier. The upper and lower bound of the distance constraints have been obtained by enhancing and reducing the derived distance by 10%. The complete set of NOE distance constraints, used for structure calculation, is shown in Supporting Information. As a first step, a mild minimization with constraints was performed in order to remove bad steric contacts. The following general protocol was used for minimizing energy. Energy minimization of each structure was first carried out by the steepest descent method followed by the conjugate gradient method until a maximum of 1000 iterations or an rms deviation of 0.001 kcal/mol have been achieved. For MD runs, a temperature of 300 K was used. The molecules were initially equilibrated for 50 ps and subsequently subjected to 1 ns dynamics with a step size of 1 fs, sampling the trajectory at equal intervals of 10 ps. In this trajectory, 106 samples were generated and were again energy minimized.

Boc-L-Ala- ϵ -Caa_(x)-OMe (10). A solution of **1** (0.32 g, 0.77 mmol) and CF_3COOH (0.32 mL) in CH_2Cl_2 (3 mL) was stirred at room temperature. After 2 h, solvent was evaporated under reduced pressure to obtain **6**, which was dried under high vacuum and used as such without any further purification. A cooled (0°C) solution of **8** (0.15 g, 0.77 mmol), HOBt (0.13 g, 0.92 mmol), and EDCI (0.18 g, 0.92 mmol) in CH_2Cl_2 (6 mL) was stirred under N_2 atmosphere for 15 min and treated sequentially with the salt **6**, DIPEA (0.2 mL, 1.16 mmol). After 4 h, the reaction mixture was cooled to 0°C , treated with saturated NH_4Cl solution (10 mL), and stirred for 10 min. The reaction mixture was diluted with CHCl_3 (20 mL), then washed sequentially with 1 N HCl (10 mL), water (10 mL), aq saturated NaHCO_3 solution (10 mL), and brine (10 mL). The organic layer was dried (Na_2SO_4) and evaporated and the residue obtained was purified by column chromatography (silica gel, 50% ethyl acetate in petroleum ether) to give **10** (0.31 g, 84%) as a white solid, mp $80\text{--}82^\circ\text{C}$; $[\alpha]_{\text{D}} -129.8$ (*c* 0.3 CHCl_3); IR (KBr) ν 3353, 2984, 2932, 1732, 1692, 1540, 1518, 1457, 1374, 1317, 1261, 1166, 1077, 1027, 901, 852 cm^{-1} ; ^1H NMR (CDCl_3 , 400 MHz) δ 6.14 (d, 1H, $J = 9.1$ Hz, NH-2), 5.89 (d, 1H, $J = 3.8$ Hz, C₁H-2), 5.11 (d, 1H, $J = 8.2$, NH-1), 4.56 (d, 1H, $J = 3.8$ Hz, C₂H-2), 4.25 (m, 1H, C_eH-2), 4.11 (m, 1H, $J = 7.2$, C _{α} H-1), 4.10 (dd, 1H, $J = 3.2$, 6.1 Hz, C₄H-2), 3.66 (s, 3H, COOMe), 3.64 (d, 1H, $J = 3.2$ Hz, C₃H-2), 3.56 (s, 3H, OMe), 2.35 (m, 2H, C _{α} H-2), 1.68 (m, 1H, C _{β} H-2), 1.58 (m, 1H, C _{β'} H-2), 1.56 (m, 1H, C _{γ} H-2), 1.51 (m, 1H, C _{γ'} H-2), 1.49 (s, 3H, Me), 1.43 (s, 9H, Boc), 1.37 (m, 2H, C _{δ} H-2), 1.32 (d, 3H, $J = 7.1$ Hz, C₃), 1.31 (s, 3H, Me); ^{13}C NMR (CDCl_3 , 100 MHz) δ 174.0, 172.1, 155.4, 111.4, 104.0, 84.7, 81.3, 80.6, 77.2, 76.7, 57.6, 51.4, 50.1, 47.7, 33.8, 32.5, 29.6, 28.3, 26.7, 26.1, 24.9, 24.6, 18.2; HRMS (ESI) m/z calcd for $\text{C}_{23}\text{H}_{40}\text{N}_2\text{O}_9\text{Na}$ ($\text{M}^+ + \text{Na}$) 511.2631, found 511.2632.

Boc- ϵ -Caa_(x)-L-Ala-OMe (11). A solution of **1** (0.23 g, 0.55 mmol) in methanol (2 mL) was cooled to 0°C and treated with aq 4 N NaOH solution (2 mL). The reaction mixture was stirred at room temperature for 2 h. Solvent was evaporated and the pH was adjusted to 2–3 with aq 1 N HCl solution at 0°C and extracted with ethyl acetate (2×10 mL). The organic layer was dried (Na_2SO_4) and evaporated under reduced pressure to afford **7** (0.21 g, 94%), which was used as such for further reaction.

A solution of acid **7** (0.21 g, 0.52 mmol) in CH_2Cl_2 (5 mL) was cooled to 0°C , then treated with HOBt (0.08 g, 0.62 mmol) and EDCI (0.12 g, 0.62 mmol); the salt **9** and DIPEA (0.13 mL, 0.78 mmol) were added as described for the synthesis of **10**. Workup and purification by column chromatography (silica gel, 50% ethyl acetate in petroleum ether) gave **11** (0.21 g, 90%) as a semisolid; $[\alpha]_{\text{D}} -28.0$ (*c* 0.25 CHCl_3); IR (KBr) ν 3362, 2983, 2937, 1756, 1695, 1652, 1525, 1458, 1385, 1260, 1171, 1076 cm^{-1} ; ^1H NMR (CDCl_3 , 500 MHz) δ 6.10 (d, 1H, $J = 7.6$ Hz, NH-2),

5.90 (d, 1H, $J = 3.9$ Hz, C₁H), 4.66 (d, 1H, $J = 9.0$ Hz, NH-1), 4.58 (m, 1H, C_αH-2), 4.55 (d, 1H, $J = 3.9$ Hz, C₂H), 4.11 (m, 1H, C_εH), 4.01 (dd, 1H, $J = 3.2, 7.1$ Hz, C₄H), 3.74 (s, 3H, COOMe), 3.62 (d, 1H, $J = 3.2$ Hz, C₃H-1), 3.36 (s, 3H, OMe), 2.21 (m, 2H, C_αH-1), 1.80–1.48 (m, 4H, C_βH, C_γH), 1.47 (s, 3H, Me), 1.43 (s, 9H, Boc), 1.42 (m, 3H, CH₃-2), 1.40–1.30 (m, 2H, C_δH), 1.31 (s, 3H, Me); HRMS (ESI) m/z calcd for C₂₃H₄₀N₂O₉Na (M⁺ + Na) 511.2631, found 511.2635.

Boc-L-Ala-ε-Caa_(x)-L-Ala-Ome (2). A solution of **11** (0.13 g, 0.26 mmol) and CF₃COOH (0.13 mL) in CH₂Cl₂ (1.5 mL) was stirred at room temperature as described for **6** to give **12**, which was used as such without any further purification. As described for the synthesis of **10**, a mixture of acid **8** (0.05 g, 0.26 mmol), HOBt (0.04 g, 0.31 mmol), and EDCI (0.06 g, 0.31 mmol) in CH₂Cl₂ (3 mL) was stirred at 0 °C for 15 min, followed by the salt **12** and DIPEA (0.07 mL, 0.39 mmol). Workup and purification by column chromatography (silica gel, 90% ethyl acetate in petroleum ether) afforded **2** (0.12 g, 82%) as a white solid, mp 79–81 °C; [α]_D –57.9 (*c* 0.25, CHCl₃); IR (KBr) ν 3309, 2982, 2934, 1718, 1650, 1543, 1455, 1373, 1215, 1167, 1083, 1023, 850 cm⁻¹; ¹H NMR (CDCl₃, 600 MHz) δ 6.93 (d, 1H, $J = 7.6$ Hz, NH-3), 6.63 (d, 1H, $J = 9.4$ Hz, NH-2), 5.89 (d, 1H, $J = 3.9$ Hz, C₁H-2), 5.29 (d, 1H, $J = 8.1$ Hz, NH-1), 4.59 (m, 1H, $J = 7.2$ Hz, C_εH-3), 4.56 (d, 1H, $J = 3.9$ Hz, C₂H-2), 4.27 (dq, 1H, $J = 3.5, 8.8$ Hz, C_εH-2), 4.09 (dd, 1H, $J = 3.0, 7.8$ Hz, C₄H-2), 3.75 (s, 3H, COOMe), 3.62 (d, 1H, $J = 3.0$ Hz, C₃H-2), 3.36 (s, 3H, OMe), 2.24 (td, 1H, $J = 6.4, 14.3$ Hz, C_αH-2), 2.19 (td, 1H, $J = 7.1, 14.0$ Hz, C_αH-2), 1.66 (m, 2H, C_βH-2), 1.53 (m, 1H, C_γH-2), 1.51 (m, 1H, C_γH-2), 1.49 (s, 3H, Me), 1.43 (s, 9H, Boc), 1.42 (m, 3H, Me), 1.39 (m, 1H, C_δH-2), 1.38–1.37 (m, 6H, CH₃), 1.36 (m, 1H, C_δH-2), 1.32 (s, 3H, Me); ¹³C NMR (CDCl₃, 100 MHz) δ 174.4, 173.1, 172.5, 155.6, 111.4, 104.7, 84.4, 84.2, 81.3, 80.9, 80.8, 79.8, 57.6, 52.5, 50.4, 47.9, 36.4, 32.0, 29.7, 28.3, 26.7, 26.2, 24.8, 18.2, 18.1, 17.9; HRMS (ESI) m/z calcd for C₂₆H₄₅N₃O₁₀Na (M⁺ + Na) 582.3002, found 582.3023.

Boc-L-Ala-ε-Caa_(x)-L-Ala-ε-Caa_(x)-Ome (3). As described for the synthesis of **7**, a solution of **10** (0.12 g, 0.25 mmol) on reaction with aq 4 N NaOH solution (1 mL) and workup furnished **14** (0.12 g, 96%), which was used as such for the next reaction. A solution of **10** (0.11 g, 0.23 mmol) and CF₃COOH (0.14 mL) in CH₂Cl₂ (1 mL) was stirred at room temperature as described for **6** to give H-L-Ala-ε-Caa_(x)-Ome·CF₃COOH (**15**), which was used as such without any further purification. As described for the synthesis of **11**, a mixture of acid **14** (0.11 g, 0.23 mmol), HOBt (0.04 g, 0.27 mmol), and EDCI (0.053 g, 0.27 mmol) in CH₂Cl₂ (3 mL) was stirred at 0 °C for 15 min followed by the salt **15** and DIPEA (0.06 mL, 0.34 mmol). Workup and purification by column chromatography (silica gel, 2% MeOH in CHCl₃) afforded **3** (0.09 g, 46%) as a white solid, mp 74–76 °C; [α]_D –129.6 (*c* 0.65, CHCl₃); IR (KBr) ν 3328, 2983, 2934, 1656, 1537, 1454, 1376, 1251, 1167, 1080, 1022, 857 cm⁻¹; ¹H NMR (CDCl₃, 600 MHz) δ 7.00 (d, 1H, $J = 7.1$ Hz, NH-3), 6.77 (d, 1H, $J = 9.6$ Hz, NH-2), 6.18 (d, 1H, $J = 9.4$ Hz, NH-4), 5.90 (d, 1H, $J = 3.8$ Hz, C₁H-4), 5.88 (d, 1H, $J = 3.8$ Hz, C₁H-2), 5.41 (d, 1H, $J = 7.9$ Hz, NH-1), 4.56 (d, 1H, $J = 3.8$ Hz, C₂H-4), 4.55 (d, 1H, $J = 3.8$ Hz, C₂H-2), 4.34 (m, 1H, C_αH-3), 4.25 (m, 1H, C_εH-2), 4.12 (m, 1H, C_αH-1), 4.06 (m, 1H, C₄H-4), 4.05 (m, 1H, C₄H-2), 3.67 (s, 3H, COOMe), 3.64 (d, 1H, $J = 3.4$ Hz, C₃H-4), 3.62 (d, 1H, $J = 3.4$ Hz, C₃H-2), 3.35 (s, 3H, OMe), 3.34 (s, 3H, OMe), 2.30 (m, 2H, C_αH-4), 2.11 (m, 2H, C_αH-2), 1.68 (m, 2H, C_βH-2), 1.65 (m, 2H, C_βH-4), 1.53 (m, 2H, C_γH-4), 1.50 (s, 3H, Me), 1.48 (m, 2H, C_γH-2), 1.43 (s, 9H, Boc), 1.42 (m, 3H, CH₃-3), 1.34 (s, 3H, Me), 1.33 (m, 3H, CH₃-1), 1.32 (s, 3H, Me), 1.31 (s, 3H, Me); ¹³C NMR (CDCl₃, 100 MHz) δ 174.1, 174.0, 173.1, 172.6, 172.2, 155.6, 111.5, 111.3, 104.7, 104.6, 84.6, 84.4, 81.3, 81.2, 81.0, 80.8, 79.7, 57.7, 57.6, 51.5, 51.3, 50.3, 50.1, 49.3, 47.9, 47.8, 36.5, 36.3, 33.8, 32.4, 32.2, 29.7, 28.4, 26.7, 26.1, 25.0, 24.8, 24.7, 18.1, 17.8;

HRMS (ESI) m/z calcd for C₄₀H₆₈N₄O₁₅Na (M⁺ + Na) 867.4578, found 867.4599.

Boc-L-Ala-ε-Caa_(x)-L-Ala-ε-Caa_(x)-L-Ala-Ome (4). As described for the synthesis of **7**, reaction of **2** (0.1 g, 0.17 mmol) with aq 4 N NaOH solution (1 mL) and workup furnished **13** (0.09 g, 98%), which was used as such for the next reaction. A solution of **11** (0.07 g, 0.14 mmol) and CF₃COOH (0.07 mL) in CH₂Cl₂ (1 mL) was stirred at room temperature as described for **6** to give **12**, which was used as such without any further purification. As described for the synthesis of **10**, a mixture of acid **13** (0.08 g, 0.14 mmol), HOBt (0.02 g, 0.17 mmol), and EDCI (0.03 g, 0.17 mmol) in CH₂Cl₂ (3 mL) was stirred at 0 °C for 15 min followed by the salt **12** and DIPEA (0.04 mL, 0.22 mmol). Workup and purification by column chromatography (silica gel, 3.0% MeOH in CHCl₃) afforded **4** (0.07 g, 56%) as a white solid, mp 85–87 °C; [α]_D –121.3 (*c* 0.2, CHCl₃); IR (KBr) ν 3423, 2928, 1653, 1543, 1456, 1378, 1260, 1166, 1083, 1023, 858, 802 cm⁻¹; ¹H NMR (CDCl₃, 600 MHz) δ 8.33 (d, 1H, $J = 7.3$ Hz, NH-5), 7.93 (d, 1H, $J = 6.7$ Hz, NH-3), 7.66 (d, 1H, $J = 9.7$ Hz, NH-2), 7.19 (d, 1H, $J = 9.7$ Hz, NH-4), 5.92 (d, 1H, $J = 3.9$ Hz, C₁H-2), 5.87 (d, 1H, $J = 3.8$ Hz, C₁H-4), 5.23 (d, 1H, $J = 7.8$ Hz, NH-1), 4.58 (m, 2H, C₂H-4, C_αH-5), 4.55 (d, 1H, $J = 3.9$ Hz, C₂H-2), 4.19 (m, 1H, C_αH-3, C_εH-4), 4.16 (m, 1H, C_εH-2), 4.11 (dd, 1H, $J = 3.1, 8.9$ Hz, C₄H-2), 4.10 (p, 1H, $J = 7.5$ Hz, C_αH-1), 4.08 (dd, 1H, $J = 2.9, 8.6$ Hz, C₄H-4), 3.74 (s, 3H, COOMe), 3.60 (d, 1H, $J = 2.9$ Hz, C₃H-4), 3.51 (d, 1H, $J = 3.1$ Hz, C₃H-4), 3.35 (s, 3H, OMe), 3.33 (s, 3H, OMe), 2.30 (td, 1H, $J = 5.0, 14.1$ Hz, C_αH-4), 2.24 (m, 1H, C_αH-2), 2.23 (m, 1H, C_αH-4), 2.17 (ddd, 1H, $J = 4.3, 10.2, 14.1$ Hz, C_αH-2), 1.61 (m, 2H, C_βH-4), 1.60 (m, 2H, C_βH-2), 1.49 (s, 3H, Me), 1.44 (m, 2H, C_γH-4), 1.43 (s, 9H, Boc), 1.42 (d, 3H, $J = 7.4$ Hz, CH₃-5), 1.39 (d, 3H, $J = 7.3$ Hz, CH₃-3), 1.36 (d, 3H, $J = 7.0$ Hz, CH₃-1), 1.31 (m, 2H, C_γH-2), 1.31 (m, 2H, C_δH-4), 1.25 (s, 3H, Me), 1.22 (m, 2H, C_δH-2); ¹³C NMR (CDCl₃, 150 MHz) δ 175.2, 174.1, 173.0, 172.9, 172.0, 155.6, 111.2, 104.6, 96.0, 83.9, 83.6, 81.3, 81.0, 80.9, 79.6, 57.4, 57.2, 52.4, 50.7, 50.2, 48.5, 47.9, 36.8, 31.8, 31.5, 31.1, 29.6, 29.3, 28.3, 27.2, 26.8, 26.7, 26.2, 26.1, 25.7, 25.5, 24.6, 22.7, 18.4, 17.6, 17.5, 14.1; HRMS (ESI) m/z calcd for C₄₃H₇₃N₅O₁₆Na (M⁺ + Na) 938.4950, found 938.4972.

Boc-L-Ala-ε-Caa_(x)-L-Ala-ε-Caa_(x)-L-Ala-ε-Caa_(x)-Ome (5). As described for the synthesis of **7**, a solution of **3** (0.07 g, 0.08 mmol) on reaction with aq 4 N NaOH solution (0.32 mL) and workup furnished **16** (0.05 g, 81%), which was used as such for the next reaction. A solution of **11** (0.03 g, 0.06 mmol) and CF₃COOH (0.03 mL) in CH₂Cl₂ (0.3 mL) was stirred at room temperature as described for **6** to give **15**, which was used as such without any further purification. As described for the synthesis of **10**, a mixture of acid **16** (0.05 g, 0.06 mmol), HOBt (0.01 g, 0.07 mmol), and EDCI (0.01 g, 0.06 mmol) in CH₂Cl₂ (2 mL) was stirred at 0 °C for 15 min followed by the salt **15** and DIPEA (0.02 mL, 0.09 mmol). Workup and purification by column chromatography (silica gel, 2.6% MeOH in CHCl₃) afforded **5** (0.03 g, 46%) as a white solid, mp 104–106 °C; [α]_D –126.2 (*c* 0.6, CHCl₃); IR (KBr) ν 3312, 2984, 2936, 1652, 1541, 1454, 1376, 1250, 1167, 1080, 1022, 857 cm⁻¹; ¹H NMR (CDCl₃, 600 MHz) δ 8.54 (d, 1H, $J = 6.4$ Hz, NH-5), 8.13 (d, 1H, $J = 6.7$ Hz, NH-3), 7.93 (d, 1H, $J = 9.0$ Hz, NH-2), 7.66 (d, 1H, $J = 9.2$ Hz, NH-4), 6.33 (d, 1H, $J = 9.4$ Hz, NH-6), 5.91 (d, 1H, $J = 3.9$ Hz, C₁H-2), 5.90 (d, 1H, $J = 3.9$ Hz, C₁H-6), 5.87 (d, 1H, $J = 3.9$ Hz, C₁H-4), 5.37 (d, 1H, $J = 7.8$ Hz, NH-1), 4.59 (d, 1H, $J = 3.9$ Hz, C₂H-2), 4.57 (d, 1H, $J = 3.9$ Hz, C₂H-4), 4.55 (d, 1H, $J = 3.9$ Hz, C₂H-6), 4.25 (dq, 1H, $J = 3.9, 9.5$, C_εH-6), 4.24 (m, 1H, C_αH-3), 4.22 (m, 1H, C_αH-5), 4.15 (m, 2H, C_εH-1, C₄H-2), 4.14 (m, 1H, C₄H-6), 4.12 (m, 2H, C_εH-4, C₄H-2), 4.11 (m, 1H, C_αH-1), 3.69 (s, 3H, COOMe), 3.63 (d, 1H, $J = 3.1$ Hz, C₃H-6), 3.58 (d, 1H, $J = 3.1$ Hz, C₃H-4), 3.49 (d, 1H, $J = 3.4$ Hz, C₃H-2), 3.35 (s, 3H, OMe), 3.34 (s, 3H, OMe), 3.33 (s, 3H, OMe), 2.35 (m, 2H,

$C_{\alpha}H-6$, 2.25 (m, 1H, $C_{\alpha}H-2$), 2.24 (m, 1H, $C_{\alpha}H-4$), 2.20 (m, 1H, $C_{\alpha}H-4$), 2.16 (m, 1H, $C_{\alpha}H-2$), 1.65 (m, 2H, $C_{\beta}H-6$), 1.64 (m, 2H, $C_{\beta}H-4$), 1.59 (m, 2H, $C_{\beta}H-2$), 1.52 (s, 6H, 3 × Me), 1.50 (s, 3H, Me), 1.44 (m, 2H, $C_{\gamma}H-6$), 1.43 (s, 9H, Boc), 1.40 (m, 2H, $C_{\gamma}H-4$), 1.39 (d, 3H, $J=7.4$ Hz, CH_3-3), 1.37 (d, 3H, $J=7.3$ Hz, CH_3-1), 1.36 (m, 2H, $C_{\delta}H-6$), 1.35 (d, 3H, $J=7.0$ Hz, CH_3-5), 1.33 (s, 3H, Me), 1.31 (s, 3H, Me), 1.30 (m, 2H, $C_{\gamma}H-2$), 1.24 (s, 3H, Me), 1.20 (m, 2H, $C_{\delta}H-2$), 1.16 (m, 2H, $C_{\delta}H-4$); ^{13}C NMR (CDCl₃, 150 MHz) δ 174.2, 174.1, 173.1, 155.6, 111.4, 111.2, 111.1, 104.8, 104.7, 104.6, 96.1, 84.3, 84.1, 83.7, 81.5, 81.4, 81.1, 81.0, 80.9, 80.8, 79.6, 57.5, 57.4, 57.3, 51.6, 50.8, 50.4, 50.1, 48.9, 48.7, 47.9, 37.2, 37.0, 36.9, 33.9, 32.1, 31.4, 31.2, 29.7, 28.4, 26.9, 26.8, 26.6, 26.3, 26.2, 26.0, 25.9, 25.8, 25.0, 24.8, 24.7, 24.4, 22.2, 18.5, 17.6, 17.3, 14.8; HRMS (ESI) m/z calcd for $C_{57}H_{96}N_6O_{21}-Na$ ($M^+ + Na$) 1223.6526, found 1223.6525.

Quantum Chemical Calculations. All quantum chemical calculations were performed employing the program package Gaussian 03.¹²

Acknowledgment. B.S. and D.C. are thankful to UGC and CSIR, New Delhi for a fellowship. P.S. and H.-J.H are

obliged to Deutsche Forschungsgemeinschaft for continuous support (Project HO 2346/1-3 and SFB 610).

Supporting Information Available: NMR details, solvent titration plots, distance constraints used in MD calculations, and details of quantum chemical calculations. This material is available free of charge via the Internet at <http://pubs.acs.org>.

(12) Gaussian 03, Revision C.02, Frisch, M. J.; Trucks, G. W.; Schlegel, H. B.; Scuseria, G. E.; Robb, M. A.; Cheeseman, J. R.; Montgomery, J. A.; Vreven, T.; Kudin, K. N.; Burant, J. C.; Millam, J. M.; Iyengar, S. S.; Tomasi, J.; Barone, V.; Mennucci, B.; Cossi, M.; Scalmani, G.; Rega, N.; Petersson, G. A.; Nakatsuji, H.; Hada, M.; Ehara, M.; Toyota, K.; Fukuda, R.; Hasegawa, J.; Ishida, M.; Nakajima, T.; Honda, Y.; Kitao, O.; Nakai, H.; Klene, M.; Li, X.; Knox, J. E.; Hratchian, H. P.; Cross, J. B.; Adamo, C.; Jaramillo, J.; Gomperts, R.; Stratmann, R. E.; Yazyev, O.; Austin, A. J.; Cammi, R.; Pomelli, C.; Ochterski, J. W.; Ayala, P. Y.; Morokuma, K.; Voth, G. A.; Salvador, P.; Dannenberg, J. J.; Zakrzewski, V. G.; Dapprich, S.; Daniels, A. D.; Strain, M. C.; Farkas, O.; Malick, D. K.; Rabuck, A. D.; Raghavachari, K.; Foresman, J. B.; Ortiz, J. V.; Cui, Q.; Baboul, A. G.; Clifford, S.; Cioslowski, J.; Stefanov, B. B.; Liu, G.; Liashenko, A.; Piskorz, P.; Komaromi, I.; Martin, R. L.; Fox, D. J.; Keith, T.; Al-Laham, M. A.; Peng, C. Y.; Nanayakkara, A.; Challacombe, M.; Gill, P. M. W.; Johnson, B.; Chen, W.; Wong, M. W.; Gonzalez, C.; Pople, J. A., Gaussian Inc., Wallingford CT, 2004.